DOI: 10.4408/IJEGE.2018-02.O-01

THE SWELLING AND SHRINKAGE PROPERTIES OF CLAY-RICH SOILS AFTER CEMENT TREATMENT: A MICROSTRUCTURAL APPROACH

Hizia BEKHOUCHE(*), Khelifa ABBECHE(*), Myriam DUC(**),
Ouassila BAHLOUL(*) & Pierre DELAGE(***)

(*)University of Batna2 - Department of Civil Engineering - Laboratory of Research in Applied Hydraulics (LRHYA) - Batna, Algeria
(**)Université Paris Est IFSTTAR/GERS/SRO - 14-20 boulevard Newton - 77447 Marne-la-Vallée cedex 2, France
(***)Ecole des Ponts ParisTech - U.R. Navier/CERMES - 6-8 av. Blaise Pascal - Cité Descartes - Champs-sur-Marne - 77455 Marne-la- Vallée cedex 2, France
Corresponding author: abbechek@yahoo.fr

EXTENDED ABSTRACT

Le proprietà geotecniche e meccaniche di tre campioni di terreni ricchi di argilla rigonfiante, prima e dopo il trattamento con varie quantità di legante idraulico, sono state spiegate utilizzando test chimico-fisici. I terreni testati hanno rilevato che SB, SM e ST provengono dalle regioni algerine di Batna, Meskiana e Timgad. I suoli contengono quantità crescenti di particelle fini inferiori a 2 μm e rispettivamente 50%, 25% e 33% di carbonati (dolomite e calcite) e 13%, 20% e 22% di montmorillonite (argilla rigonfiante). Per stabilizzare la deformazione del terreno sotto la variazione di umidità, su ciascun terreno è stata applicata un'aggiunta di 1%, 3%, 5%, 7% o 9% di cemento Portland (CPJ - CEMII / A 42,5 con clinker> 65%). Poiché la microstruttura del suolo governa il comportamento meccanico o idraulico del suolo stesso, la microscopia elettronica a scansione ambientale (SEM), la porosimetria a intrusione di mercurio (MIP) e la diffrazione a raggi X (XRD) e l'adsorbimento della molecola blu di metilene (*Vbs*) sono stati utilizzati per spiegare il cambiamento dell'organizzazione delle particelle del suolo e la mineralogia, dopo l'aggiunta di cemento. Considerando che la preparazione del campione influisce fortemente sulla microstruttura del suolo e sullo sviluppo di C-S-H durante l'idratazione del cemento, il processo utilizzato per la compattazione dinamica o statica e varie dimensioni degli aggregati del terreno è stato accuratamente dettagliato. Dopo l'aggiunta del cemento, i terreni naturali sono stati compattati e preparati per il *Proctor test*, mentre i terreni finemente macinati sono stati miscelati con il cemento, prima della compattazione statica, per prove di taglio o di rigonfiamento e contrazione. A livello globale, la microstruttura del suolo è cambiata sia sotto l'effetto flocculante a breve termine indotto dall'aumento del contenuto di calcio nel suolo (calcio che viene rilasciato durante l'idratazione del cemento), sia dall'effetto a lungo termine dei prodotti precipitati durante la presa del cemento (effetto legante). La riduzione del *Vbs* (un parametro correlato alla superficie dell'aggregato del suolo) è stata principalmente attribuita all'effetto flocculante del Ca^{2+} che ha contribuito anche alla leggera diminuzione delle densità ottimali γ_{dOPN}, mentre il contenuto d'acqua ottimale Proctor w_{OPN} è aumentato con l'aggiunta di cemento. Le misurazioni MIP hanno confermato l'effetto flocculante del cemento sul terreno dalla scomparsa dei micropori e l'aumento dei pori con dimensioni inferiori. Contrariamente al MIP che rileva i composti cementizi con la loro nanoporosità, la mineralogia dei terreni dopo l'aggiunta di cemento non ha chiaramente dimostrato né la presenza di nuove fasi cristalline, né di quelle amorfe. Il basso tenore di CSH nei terreni trattati con cemento ha spiegato in parte tali risultati, specialmente perché il breve tempo di indurimento (28 giorni) non ha favorito le reazioni pozzolaniche tra argilla e cemento, all'origine del CSH additivo che porta al rinforzo a lungo termine del suolo. Parallelamente, il trattamento del cemento ha migliorato le caratteristiche geotecniche e meccaniche dei terreni, in particolare la resistenza al taglio e la capacità portante. Infatti, i valori di coesione *c'* e l'angolo di attrito φ' sono aumentati dopo il trattamento con cemento fino ai valori massimi. Questi valori vengono raggiunti per un contenuto di cemento ottimale intorno al 7-8%. Le indagini sperimentali hanno evidenziato anche una riduzione sia dei potenziali di rigonfiamento S che delle pressioni di rigonfiamento σ_s. Un trattamento del cemento al 9% ha ridotto il potenziale di rigonfiamento del 75-91% per i terreni testati, il che corrisponde a una diminuzione della pressione del gonfiore del 70-81%. Questo comportamento concorda con l'aumento del limite plastico PL e del limite di ritiro w_S quando il cemento viene aggiunto al suolo, mentre il limite liquido LL e l'indice di plasticità IP diminuiscono. Per confermare il comportamento del potenziale di rigonfiamento *S* che dipende dal contenuto d'acqua iniziale dei terreni testati, è stato misurato un parametro più intrinseco del terreno, individuato nella deformazione totale del terreno (S_{tot}) che corrisponde alla deformazione di ritiro durante l'essiccazione dei campioni sottoposti precedentemente ad un rigonfiamento. Sia *S* che S_{tot} decrescono con la quantità di cemento nel terreno. Inoltre, le curve *S*, S_{tot} e σ_s rispetto al cemento aggiunto potrebbero essere approssimate da una equazione polinomiale di terzo ordine correlata alla posizione di due limiti osservati sulle curve w_s (o PL) rispetto alla percentuale di cemento aggiunto. Questi due limiti hanno contribuito a distinguere tre zone di rigonfiamento. La zona I corrisponde ad un aumento significativo del limite di ritiro con un elevato potenziale di rigonfiamento, ma l'aggiunta di cemento non ha ancora svolto il suo ruolo di stabilizzatore. La zona II corrisponde ad un plateau dove il limite di ritiro aumenta leggermente, accompagnato da una leggera riduzione del rigonfiamento. Questo è l'inizio dell'effetto stabilizzatore del cemento. La zona III mostra un nuovo significativo aumento dei limiti di ritiro. Il rigonfiamento si riduce a zero con il rafforzamento della struttura. Il tenore di cemento ottimale osservato in precedenza intorno al 7-8% corrisponde al limite tra le zone II e III. Da tale limite è stata raggiunta una massima coesione *c'* e l'angolo di attrito φ'. Corrisponde anche, per il suolo SB, alla stabilizzazione del decremento del contenuto d'acqua massimo w_{max} o *Vbs*.

ABSTRACT

The properties of three expansive clay-rich soils from Algeria, before and after treatment with various quantities of cement was explained using physico-chemical tests. SEM, MIP and XRD as well as the adsorption of methylen blue molecule (Vbs) were carried out to observe the microstructure change under both the short term flocculating effect of Ca^{2+} and the long term effect of precipitated products during cement hydration (binding effect). The flocculating effect contributed also to the change of proctor optimum characteristics: $\gamma_{d,OPN}$ decreased while w_{OPN} increased with the cement addition. As expected, experimental investigations evidenced a reduction of both the swelling potentials S, the total soil deformation S_{tot} and the swelling pressures σ_s when the amount of cement increased. S, S_{tot}, σ_s and the shrinkage limit w_s (or the liquid limit LL) versus the added cement followed a third polynomial curve, allowing to establish three swelling zones. An optimum cement content around 7-8% corresponded to the limit between zone II and III. From such limit, a maximum cohesion c' and friction angle ϕ' was reached which corresponded to a significant improvement of mechanical characteristics, while the decrease of Vbs or the maximum water content w_{max} stopped.

***Keywords**: swelling, shrinkage, cement treatment, expansive clays, microstructure*

INTRODUCTION

Major disorders caused by swelling soils have been observed in arid and semi-arid areas all over the world (Chen, 1988; Nelson & Miller, 1992; Nalbantoglu & Gucbilmez, 2001; Al-Mhaidib, 2006). In these areas, the climate is characterized by low precipitation and significant difference of temperature between winter and summer, with cold wet winter and warm dry summer. Furthermore, their geology is often characterised by the presence of clay rich geological formations that exhibit large volumetric changes when the climatic conditions vary. This is particularly true during long drought periods, or when human activities affect the groundwater level, due either to excessive pumping for irrigation in agriculture or to the development of industries or urbanization. So, the swelling-shrinkage phenomenon that affects soils and foundations of houses, roads or embankments, requires special attention from geotechnical engineers. The soil stabilization is usually obtained by the use of higher quality materials for construction (but with additional costs), or by the use or reuse of local materials, including expansive soils after a stabilizing treatment especially with cement or lime. The treatment allows better soil compaction by reducing the soil plasticity and, consequently, by improving its bearing capacity. Improvement methods of swelling soils also include the addition of sand (Louafi & Bahar, 2012), of salt (Bekkouche *et alii*, 2007; Belabbaci *et alii*, 2013; Hachichi *et alii*, 2007), or of a mix of dune sand and salt (Lamara *et alii*, 2006). But the efficiency of these treatments has not yet been clearly demonstrated in practice, contrary to cement and/or lime treatments.

The soil stabilization by using cement and/or lime has been investigated by numerous authors (Petry & Little, 2002). Most authors showed that adding various proportions of lime or cement resulted in a reduction of both the swelling potential S and the swelling pressure σ_s of expansive soils. Al-Rawas *et alii* (2005) demonstrated on expansive soils from Al-Khod Omen that an lime addition of 6% reduced S and σ_s to zero, while more surprisingly, a 6% or 9% treatment with Sarooj (an artificial pozzolan) resulted in an increase in swelling pressure. Gueddouda *et alii* (2013) investigated the effects of salts, lime, cement, lime/cement or lime/salt mixtures, and evidenced a reduction of the swelling potential of 70% with the lime/cement mixture, and of 80% with the lime/salt one.

The treatment with chemical stabilizer usually reaches a maximum effect above a given amount, as for example 6% or 8% of lime for Al-Rawas *et alii* (2005) and Derriche & Lazzali (1997) respectively, or 3% to 6% of lime for Mellas *et alii* (2012). The swelling properties and bearing capacity of treated expansive soils are improved by reducing the clay sensitivity to water, in link with the reduction of the plasticity index (PI). The fluctuant behavior of PI observed by Al-Rawas *et alii* (2005) indicated a more complex impact of the stabilizer. PI initially increased after a 3% lime or cement treatment, or a lime/Sarooj mixture at 3% for each component, while other additions induced a gradual decrease of PI. In contrast, the 3% or 5% lime-3% cement treated specimen presented an initial reduction of PI followed by a general increase.

Among other studies, the Mahamedi and Khemissa's works (Mahamedi & Khemissa, 2013; Khemissa & Mahamedi, 2014; Khemissa *et alii*, 2017 or 2018) focused on soils close to the Aures region in Algeria, whose geology is close the one where the soil specimens tested in the present study have been extracted. Lamara & Gueddouda (2008) showed that Algerian natural clayey soils are globally over-consolidated, have low permeability and do not exhibit significant creep. The over-consolidation is due to shrinkage and results in a significant desiccation of the soils. The present paper aims to validate and complete the results previously published by especially Khemissa *et alii* (2017, 2018) who experimentally investigated the behavior of an over-consolidated swelling clay, in intact and compacted state

Not only the swelling behaviour has to be studied but also the shrinkage one. If the swelling phenomenon is systematically considered in engineering study applied on expansive soils, their shrinkage behaviour is less investigated because of the usual dry state of soils in arid regions. Nevertheless, damages occur after a

succession of swelling and shrinkage so the shrinkage properties of soil have to be also considered as well as the effect of wet-dry cycles in further step. Among the rare study concerning the shrinkage phenomenon, the highly consolidated natural clay tested by Khemissa *et alii* (2018) showed not only a very high swelling pressure σ_s and free swelling S but also a very high conventional and effective shrinkage limits. But no shrinkage curve was drawn.

The present study wants to complete previous results on Algerian expansive clays by studying shrinkage and by coupling the mechanical and hydric properties of expansive soils after cement treatment and its microstructure with quantitative mineralogy and porosity measurement. The behaviours of compacted expansive clays extracted from three urbanized sites of the Aures region were compared, including the measurement of the compaction energies at the Proctor optimum, the swelling potential and swelling pressure as well as the description of the shrinkage curve after swelling, which allow the determination of the total soil deformation. Results from each test were discussed based on the soil microstructure observed by means of scanning electron microscopy, mercury intrusion porosimetry and mineralogical/chemical analysis.

MATERIALS AND METHODS

Origin of tested materials

The three tested soils were extracted in different urbanized sites. Geological maps indicate that the majority of the studied sites are composed of clay-rich or marl-rich formations with the presence sometimes of clayey-marly limestone with various colours that may be locally mixed with sand, pebbles, limestone, gypsum or silt.

The first soil was brought from the town of Timgad, located at 36 km east of the District of Batna, the capital of the Aures region. Collected at a depth of 2-4.5 metres, the Timgad soil (noted ST) is an intact marl or clay with a greenish to yellowish colour. The second sample (noted SB) was collected at a depth of 1.5 to 3 m in the town of Bitam, at approximately 80 km south-west of the District of Batna. Its geological description corresponds to intact clay or marl, with the presence of gypsum crystals. It is characterized by a yellowish to brownish colour with whitish areas. Finally, the third soil (noted SM) came from the town of Meskiana in the wilaya of Oum El Bouaghi, located in the northeast part of the Aures region. The geological characteristics of the SM sample, collected between 1.2 and 2.8 metres deep, corresponds to intact calcareous marl or clay. Its colour varies from brown to grey.

The cement mixed with soils was a Portland cement (CPJ - CEMII / A 42.5 with a minimum of 65% of clinker) manufactured locally by the AinTouta Batna cement company (Algeria). The cement characteristics given by the supplier are summarized in Tab. 1.

Geotechnical identification tests

The Atterberg limits according to the French standard NF P94-051 (1993) were measured on the soil fraction lower than 400 µm, extracted by wet sieving from untreated soils. In order to measure the consistency limits on the soil-cement mixtures, the natural soil fraction was air-dried (after the wet sieving) and mixed with different quantities of anhydrous cement powder in order to reach 1 to 9% cement addition such as during the soil treatment. After mechanical mixing during 20 min for homogenization, water was added in various quantities and the mixer was run during 5-7 min before applying the standardized method to measure Atterberg limits.

The methylene blue test was also carried out by following the procedure detailed in the French standard NF P 94-68 (1998). Raw materials were previously dried at 105°C and ground (or disaggregated) at grain size smaller than 80 µm. Then, methylene blue values were measured on ground soils mixed with anhydrous cement powder in order to simulate the 1 to 9% of cement added during the soil treatment.

Preparation of soil specimens

After soil excavation, a standard Proctor test (according to the French standard NF P 94-93 - 1999) was carried out to determine the Proctor optimum density γ_{opt} and optimum water content w_{opt} for raw soils and soil-cement mixtures with 1%, 3%, 5%, 7% and 9% cement. The parameters from the Proctor tests (given in Tab. 5) were used to prepare specimens for direct shear test, free swelling test, free swelling test followed by shrinkage test and microscopic observations. First, a required amount of finely ground soils at 80 µm after a drying at 105°C during 24 h, and various cement contents (1%, 3%, 5%, 7% and 9%) were carefully mixed in dry state during 10 min in a pale mixer to achieve satisfactory homogeneity. Then, the mixture was moistened with a quantity of tap water, in order to reach wopt determined by the Proctor tests carried out on each cement-soil mixture. The wet cement-soil mixtures were blended mechanically during 5 min (until the disappearance of cement powder in the mixture) prior to be submitted to static compaction under 50 kPa at a constant deformation rate of 1 mm/min in a cylindrical mould (70 mm in diameter and 20 mm in height). The specimens reached the maximum dry density γ_d permitted by the press. Once compacted, they were cut to reach a 20 mm height and sealed and waxed to allow for an endogen cure of 28 days prior to

Characteristics	Parameters	Results
Physical characteristics	Specific weight (g/cm^3)	3.06
	Specific surface Blaine (cm^2/g)	428
	Consistence (%)	0.35
	Curing time (h:mn)	2:02
Chemical characteristics	SiO_2: 23.5 %, Al_2O_3: 5%, Fe_2O_3: 4.2%, CaO: 56.5%, MgO: 1.8%, K_2O: 0.96%, Na_2O: 0.8%, SO_3:2.6%, CaO_{libre}: 0.94%, LOI (1000°C): 4.75%	

Tab. 1 - Cement properties

testing. This procedure was also applied on soil without cement in order to have a reference with 0% of cement.

Mechanical and hydric tests

Shear tests were carried out on treated and untreated samples, using direct shear apparatus according to French standard NF P 94-071-1 (1994). The samples were prepared in the same way as for the swelling tests in a ring with a diameter of 60 mm and a height of 21 mm.

Free swelling tests were carried out by soaking compacted and/or cement-treated specimens in oedometer cells following ASTM D 4546-96. The change in height of the samples was monitored during wetting until stabilization after several days, when the specimen reached the maximum water content. The swelling potential $S=\Delta H/H_0$ was then calculated (H and H_0 are the maximum and initial heights of the specimen, respectively). The swelling pressure P_s (%) was determined by applying increasing loading on the swelled sample, until it came back to its initial volume.

Finally, other specimens were submitted to free swelling, followed by a free shrinkage under ambient conditions. From the maximum water content w_{max} corresponding to the swelled state, the specimen weight and volume (calculated from careful measurements of sample height and diameter with a calliper) were monitored during air-drying. This allowed to draw the shrinkage curve and to calculate the total volume deformation of the sample corresponding to the change of water content from w_{max} to zero water content. The shrinkage limits of specimens were also determined, as the water content below which the sample volume remained constant. It corresponds to the physical shrinkage limit and not to the conventional one as described in standardized method.

Mineralogical analysis

Mineralogical analysis by X-ray diffraction (XRD) was obtained using a D8 advance diffractometer (Bruker) equipped with a Co anode, no monochromator and a rapid Lynx eye detector. Data were acquired with a step of 0.01° 2 theta and 1s per step. Mineral phases were analysed using Eva software coupled with ICDD-Pdf2 mineralogical data base and quantitative analyses were obtained using TOPAS software (Bruker) based on Rietveld method. Soil sample before or after cement treatment at the end of the curing period were freeze dried and ground at 80 µm with lab planetary tungsten ball mill. Front loading was applied to fill the sample holder for XRD analysis and to prevent preferential orientation of clay particles, the powder was sieved in the sample holder and the uncompacted sample surface was cut with a thin razor blade.

Microstructure analysis

The porosity of compacted soil samples was measured by mercury intrusion porosimetry (MIP) using an Autopore IV from Micromeritics. Obtain on freeze dried samples, data were collected with 10s and 30s equilibrium times at low and high pressure, respectively. Environmental scanning electron microscopy (ESEM) observations were made with a Quanta 400 microscope (from FEI) coupled with chemical EDX analyser (from EDAX) on freeze dried specimens after the 28 days of curing in hermetic conditions. A fresh fractured surface perpendicular to the compaction direction was observed in low vacuum mode (around 2% of relative humidity was imposed in the ESEM chamber).

EXPERIMENTAL RESULTS

Geotechnical characterization and classifications of raw soils

The physical characteristics of the three studied soils are given in Tab. 2. The soils noted SB (from Bitam), SM (from Meskiana) and ST (from Timgad) have a clay fraction (%< 2 µm) of 31%, 53% and 62%, respectively, with almost all the particles smaller than 2 mm. The fraction smaller than 80 µm followed the same trend as the clay fraction (the highest content is obtained in soil ST and the lowest one in soil SB).

Soil parameters	Method or standards	SB	SM	ST
Liquid limit LL (%)	NF P94-051 (1993)	68.1	82.5	95.3
Plastic limit PL (%)		26	32.7	36.6
Plasticity index PI (%)		42.1	49.8	58.7
≤ 2 mm fraction (%)	NF P94-056 (1996)	94.7	96.2	97.4
≤ 80 µm fraction (%)		70.8	82.5	95.1
≤ 2 µm fraction (%)	NF P94-057 (1992)	31	53	62
Activity of clay (Ac)	Ac = PI / (≤ 2µm)	1.35	0.93	0.94
Methylene blue value Vbs (g/100g)	NF P 94-68 (1998)	10.5	13.5	15.3
Estimation of the specific surface SSA (m^2/g)	SSA =21xVbs	220	283	321
$CaCO_3$ content (%)	NF P94-048 (1996)	58	30	29
Classifications of expansive soils (swelling potential)	SEED *et alii* (1962)	high	high	very high
	WILLIAMS & DONALDSON (1980)	very high	very high	very high
	BRE-UK (1980)	high	high	very high
	SNETHEN *et alii* (1980)	high	very high	very high

Tab. 2 - Geotechnical characterization and classification of natural intact soils (γ_s = 27 kN/m³)

Specimen parameters	Method or standards	SB	SM	ST
Natural water content w_{nat} (%)	NF P94-050 (1995)	26.4	22.5	19.3
Natural dry unit weight γ_d (kN/m^3)	NF P94-053 (2014)	14.9	16	16.6
Natural void ratio e (intact state)	$e = (\gamma_s / \gamma_d) - 1$	0,81	0,69	0.62
Natural wet unit weight γ_h (kN/m^3)	$\gamma_h = \gamma_d(1+w)$	18.8	19.6	19.8
Optimum water content w_{opt} (%)	Standard Proctor test NF P94-093 (2014)	20.5	19.8	20.8
Maximum dry density $\gamma_{d,opt}$ (kN/m^3)		16.2	16.6	16.8
Degree of saturation S_r (%) at Proctor optimum	$S_r = w/w_{sat} = w \times \left(\frac{1}{\gamma_d} - \frac{1}{\gamma_s}\right)^{-1}$	83.0	85.3	92.5
Saturation water content w_{sat} (%) at Proctor optimum	$w_{sat} = w / S_r$	24.6	23.2	22.4

Tab. 3 - Geotechnical characterization of natural intact soil (γ_s=27 kN/m^3)

Both the changes in plasticity index and methylene blue value are satisfactorily correlated to the clay fraction, with largest values for soil ST and smallest ones for soil SB. SM and ST soils have comparable activity (*Ac*) indicating comparable clay mineralogy, while soil SB exhibits a higher activity, even though having the lowest clay content. Unsurprisingly, the carbonate content follows an inverse trend compared to that of the clay fraction.

According to the French classification for fine-grained soils (NF P 11-300, 1992), the tested soils belong to subclass A4 (PI > 40 or Vbs > 8) with the presence of clays or highly plastic marly clays. To classify the soil sensitivity to swelling phenomenon, the liquid limits LL and plasticity indexes PI of each soil were reported in the Dakshanamurthy & Raman (1973) and Chen (1988) classifications superimposed to the Casagrande diagram as suggested by Khemissa *et alii* (2014). Soils are classified as highly plastic clays with high to very high swelling potentials. Results agreed with the soil classifications in Tab. 2, where soils SB and SM have a high or very high swelling potential, while soil ST has a very high swelling potential. This would indicate the predominance of montmorillonite minerals in the clay fraction.

Even if the clay fraction content slightly increases when comparing soil SB (94.7%), SM (96.2%) and ST (97.4%), the soil specimens have quite similar Proctor optimum water contents (w_{opt}) close to 20%, while the maximum dry density ($\gamma_{d,max}$) slightly increases from 16.2 kN/m^3 (SB) to 16.8 kN/m^3 (ST), as seen in Tab. 3. Remoulding and compaction carried out for the Proctor test, apparently erase the differences between the three soils in natural state, for which w_{nat} and void ratio decreased, while γ_d as well as γ_h increased. The degree of saturation at Proctor optimum varied from 83% to 85.3% and 92.5% for soils SB, SM and ST, respectively.

Mineralogy and chemistry of the soil specimens before and after cement treatment

X-ray diffraction analysis of the three soils (SB, SM and ST) without cement treatment (Fig. 1) indicates that the main minerals detected are montmorillonite $(Al_{2-x}Mg_x)Si_4(O_{10})(OH)_2(Na_{,0.5}Ca,K\ldots)_X$ (main peak at d=10-14Å), calcite ($CaCO_3$ - main peak at 3,03 Å), quartz (SiO_2 - main peak at 3,34 Å) and kaolinite ($Al_2Si_2O_5(OH)_4$ - main peak at 7 Å). The tested soils

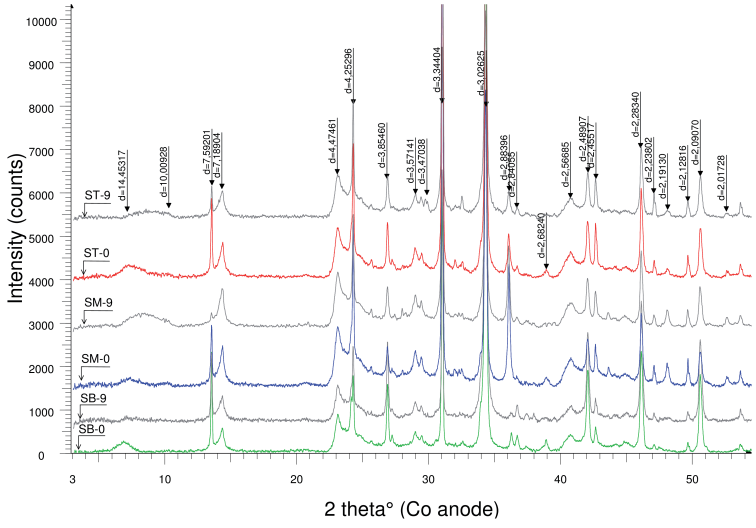

Fig. 1 - X ray diffraction patterns on untreated soils (SB-0, SM-0 and ST- 0) and on 9% cement treated soils (SB-9, SM-9 and ST- 9) after 28 days of curing after static compaction

presented similarities with clay-rich soils studied by Khemissa *et alii* (2017). Nevertheless, these authors proposed only a semi-quantification based on XRD peaks area which limits the comparison with our quantitative results. Indeed, the peak areas on XRD pattern are usually not correlated to the mineral phase quantity especially in the case of clays. The quantification of phases using Rietveld's method in Tab. 4 provides accurate mineralogical data.

The soil SB (with the lower PI, Vbs and clay fraction) exhibits the highest quantity of calcite (49.7% that is higher than 30% fixed as defining threshold for marl definition) and the lowest total amount of clay, while soils SM and ST only contain 19.9 and 29.9% of calcite, respectively. The presence of dolomite ($MgCO_3$ - main peak at d=2,88 Å) as well as calcite in soils SM and ST is observed. The quartz proportion (a well crystallized phase at the origin of XRD peak with the highest height) is lower in soil SB (11.6%) while it reaches 18-19% in soils SM and ST. The montmorillonite content is almost twice larger between soil SB and, soils SM and ST. The low values of Rwp factor (lower than 10 in Tab. 4) indicated a good confidence level in quantification (Rwp is associated to the quality of the fit by Rietveld method). Nevertheless, the total amount of clays calculated from XRD quantification appeared lower than the clay fraction (< 2 µm) from sedimentation test above all for SM and ST soils. It suggested that fine particles other than clays composed the fraction lower than 2 µm.

Other components were detected, including anatase (a titanium oxide), traces of feldspars (albite and microcline) and gypsum ($CaSO_4$, 2 H_2O - main peak at d=7,59 Å). At high level, gypsum is usually considered as a destabilizing agent of the cement hydration which impacts the soil treatment and causes the lowering of final treated soil performance. But, gypsum is also usually present at lower level as an additive in cement powder in order to slow hydration by favouring the occurrence of primary ettringite.

Finally, the presence of a low content (around 1-7%) of illite/muscovite clay minerals ($Al_{1,75}Rx$) $Si_{3,5}$ $Al_{0,5}$ $(O_{10})(OH)_2K_{0,75-1}$

Minerals	SB-0%	SB- 9%	SM-0%	SM-9%	ST-0%	ST-9%
Quartz (%)	11.6	10.5	19.1	18.5	18.7	21.2
Calcite (%)	49.7	57	19.9	25.8	29.2	29.7
Dolomite (%)	--	--	5.06	7.51	3.54	2.86
Gypsum (%)	4.4	3.48	3.99	1.96	2.43	1.69
Albite (%)	0.65	0.51	1.35	0.53	1.88	2.31
Microcline (%)	1.56	0.74	2.78	1.42	2.04	1.30
Anatase (%)	1.52	0.9	1.95	1.37	1.60	1.55
Kaolinite (%)	14.3	14.9	19.4	11.8	13.2	11.9
Muscovite/illite (%)	2.54	1.67	6.28	5.15	5.23	5.68
Montmorillonite (%)	13.6	10.7	20.2	25.9	22.3	21.7
Total amount of clays	***30.4***	***27.3***	***45.9***	***42.85***	***40.7***	***39.3***
*≤ 2µm fraction (%) **	*31*	*- - -*	*53*	*- - -*	*62*	*- - -*
Crystallinity (%)	***74.2***	***73***	***70.3***	***71.3***	***75.2***	***73.3***
Rwp	***5.33***	***5.05***	***4.97***	***4.45***	***4.94***	***4.48***

*Tab. 4 - Mineralogical composition given by XRD on compacted untreated soils and compacted cement-treated soils at the end of the 28 days of curing (Rwp: factor associated to quality of the fit). The crystallinity represents the ratio between the area of XRD peak related to crystallized phases and the area under the baseline. * NF P94-057 (1992)*

Atomic % (EDX)	SB-0%	SB- 9%	SM-0%	SM-9%	ST-0%	ST-9%
C	12.25	14.74	8.4	9.15	10.78	13.10
O	67.66	66.32	70.72	70.49	68.2	67.3
Na	0.24	0.19	0.3	0.21	0.24	0.31
Mg	0.57	0.52	0.58	0.65	0.72	0.72
Al	4.33	3.53	5.61	4.98	4.85	3.99
Si	8.84	7.2	10.13	9.36	10.21	8.43
S	**0.17**	**0.53**	**0.2**	**0.45**	**0.22**	**0.41**
K	0.63	0.28	0.54	0.35	0.44	0.36
Ca	**4.15**	**5.85**	**2.14**	**3.27**	**2.99**	**4.33**
Ti	0.1	0.11	0.18	0.12	0.18	0.12
Fe	1.05	0.73	1.2	0.98	1.16	0.91

Tab. 5 - Chemical composition (semi-quantification) by EDX coupled to ESEM observations on fresh-fractured surface of compacted untreated soils and compacted cement-treated soils at the end of the 28 days of curing

(main peak at d=10 Å) was not clearly identified on the powder pattern because of small peaks, but it was evidenced by a better fit of XRD pattern by Rietveld's method (notably the peak at d=4.47 Å). The low amount of K measured by EDX coupled with ESEM in Tab. 5 confirms the low content of illite/muscovite. Globally, XRD pattern of the three soils are quite close, as well as their chemical composition (Tab. 5). Soils are mainly composed of Al, Si Ca and Fe with low content of Mg and Na, which corresponds to the main components of clay and feldspars, as well as quartz (for Si). S and Ti were also detected because of the presence of large particles of gypsum ($CaSO_4$) observed by ESEM. Celestine (Ca, Sr)SO_4 was also observed locally, as well as the presence of titanium oxides.

After cement treatment (with CEM II/A), the chemical composition showed an increase in Ca content with the formation of hydrated products (such as C-S-H) as well as a slight increase of S that comes from the presence of gypsum in the soils before treatment, and from the gypsum intake or the formation of ettringite after cement hydration. C-S-H or ettringite were not clearly observed on XRD patterns because of their amorphous state and/or low content. Furthermore, the preparation of the soil specimen with finely ground soil (less than 80 µm) and its intimate mixture with dry cement powder before water addition, also impacts the development of the C-S-H phases, as demonstrated on lime treated soils by Wang *et alii* (2017). A similar effect is expected on the cement-treated soil studied in this paper. In other words, the specimen preparation may impact the soil reactivity in contact with cement, its microstructure and the development of detectable C-S-H.

XRD measurements in Tab. 4 demonstrated that gypsum systematically decreased after cement treatment, probably because of its high solubility and incorporation in cement products. Globally, the Si and Al contents decreased, as confirmed by a slight decrease of the quartz fraction (except for ST) and of the total amount of clays, because of the dilution effect when cement is introduced. The amount of other chemical elements in Tab. 5 remained quite constant before and after treatment which agreed with Khemissa *et alii* (2017)'s results.

After 28 days, hydration of cement occurred and the carbonation should be prevented by the curing conditions in hermetic bags. However, the carbon content increased for each tested soil after cement treatment. Carbon content may come from carbonates initially present in soils, but also from contamination by CO_2 adsorbed on surface during EDX analysis or from carbonation. XRD measures in Tab. 4 seem to validate the hypothesis of small cement carbonation, because of a systematic increase of the calcite content after cement treatment. Finally, pozzolanic reactions could also happen in presence of cement, and of clays or amorphous silica (in other words in presence of available Si source) but this phenomenon usually takes place at long term (after 28 days). However, the beginning of the pozzolanic reactions explains that the clay content diminished after treatment (parallel to the dilution effect by cement addition in soil). The slow change in mineralogy is reinforced by the slow reactivity of CEMII/A that contains blast furnace slag, activated by the dissolved clinker phases.

Effect of cement treatment on the soil microstructure

The microstructure of the statically compacted specimen (natural soil) was observed first at low magnification by environmental SEM. The fresh fractured surface of soil ST perpendicular to the compaction direction showed a more visible layered structure with the most compact microstructure, compared to both other soils. This is related to both the highest clay fraction and montmorillonite content of soil ST compared to the other soils. In the three soils, large particles embedded in a fine and compact clay-rich matrix were observed, with a higher fraction of particle larger than 80 µm in soil SB.

After cement treatment, the three soils presented similar microstructures observed at higher magnification (Fig. 2). The differences between untreated and 9% cement treated soils were most obvious in soil SM, that also exhibited a rather compact and plane surface (Fig. 2b) compared to untreated soil (Fig. 2a). The clay particles aggregated in small expansive clusters, creating a rough surface in untreated soil, disappeared after cement treatment with more compact and rigid surface with typical micro-cracks (Fig. 2b) probably induced by immersion into liquid nitrogen before the freeze-drying. The thin cracks network was observed in cement treated soils but not in untreated specimens. At higher magnification (Fig. 2 d,e), a microstructure close to the initial clay microstructure was still observed, above all in mixtures with low cement content. It indicated a probable heterogeneous repartition of cement hydrates at particle scale. The flocculated clays (because of Ca^{2+} effect) with larger pores were not distinguished as proposed by Chew *et alii* (2004) or by Osula (1996) and Khattab *et alii* (2007) when lime treatment is applied. The presence of cement hydrates such as C-S-H, C-A-H, C-A-S-H mainly under gels form was not clearly observed on ESEM images after 28 days of curing (in accordance with XRD results) except locally on the coarser soil SB, where small acicular particles associated to reticulated cement-clay structure (see circled areas in Fig. 2e) were observed as described by Kamruzzaman *et alii* (2006) and Horpibulsuk *et alii* (2010).

To complete the observation, a quantitative investigation of the effect of cement treatment is carried out by means of mercury intrusion porosimetry (MIP). Untreated soils SM and ST presented on Fig. 3a had a common bimodal porosity, with pore populations ranging between 3350 and 418 nm for micropores and 45 and 60 nm for nanopores. Untreated soil SB

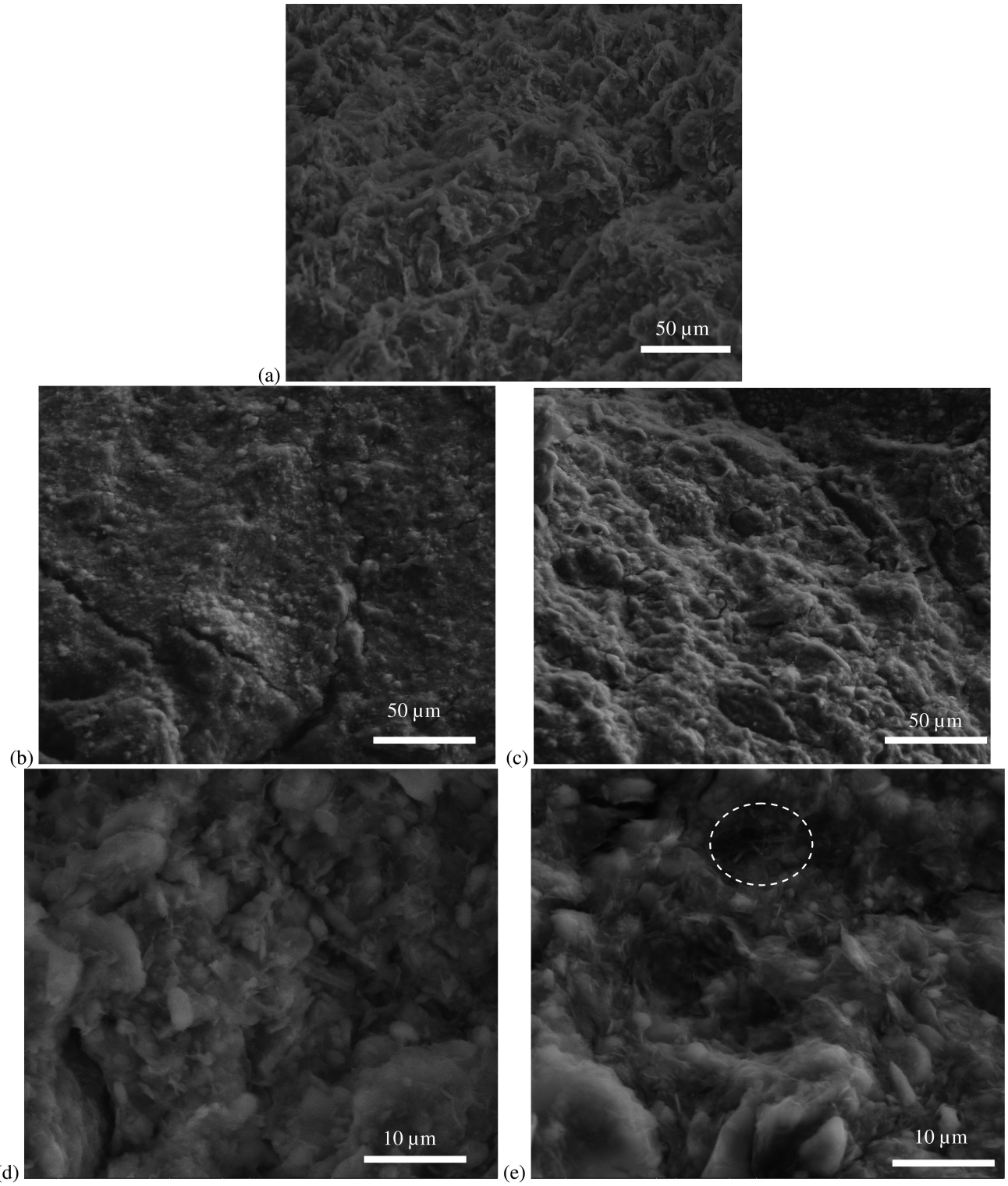

Fig. 2 - ESEM images (secondary electron images in low vacuum mode) on soil SM (x1200) (a) without treatment, (b) and (c) with cement treatment at 9%, and on soil SB (x6000) (d) without treatment, and (e) with cement treatment at 9%

exhibited a single but widespread pore population from 10 to 3400 nm. Differences were probably induced by differences in particles size distribution of soils and by small changes during static compaction. After cement treatment, the pore populations changed into two separated pore ones, in the three treated soils, with the first family centered at 1450 nm and the second one at 80 µm (Fig. 3a).

We defined here from the cumulative pore size distributions (PSD) curves presented in Fig. 3b three populations of pores, nanopore, micropores and macropores, with diameters between 10-350 nm, 0.35-10 µm and 10-300 µm, respectively. Note that that the 10 µm limit is significantly larger than the 50 nm often adopted as limit between micropores and macropores in concrete. Macropores between clusters (made up of aggregates) and that contain free water, were not observed in the specimens after static compaction. It seems that previous dry mixing between cement and finely ground soil particles prevents the appearance of macropores, usually observed in in-situ cement treated soils. Furthermore, the fractures observed in SEM images after soil freezing in liquid nitrogen did not seem to enhance the appearance of macropores. Micropores (containing mainly capillary water) correspond to inter-aggregates pores, while nanopores are related to the intra-aggregates porosity.

The PSD of the 3 soils treated with 9% of cement were really similar, with obvious micropores and nanopores. Compared to initial specimens, the microporosity was drastically reduced while the nanoporosity increased (Fig. 3b). The increase of the smallest nanopores around 10-20 nm can be related to the presence of cementitious compounds (Lemaire *et alii*, 2013). The presence of clays mixed with C-S-H is probably at the origin of the increase and shift of small nanopores toward larger sizes until 80 nm.

All the soils with or without cement treatment exhibited a

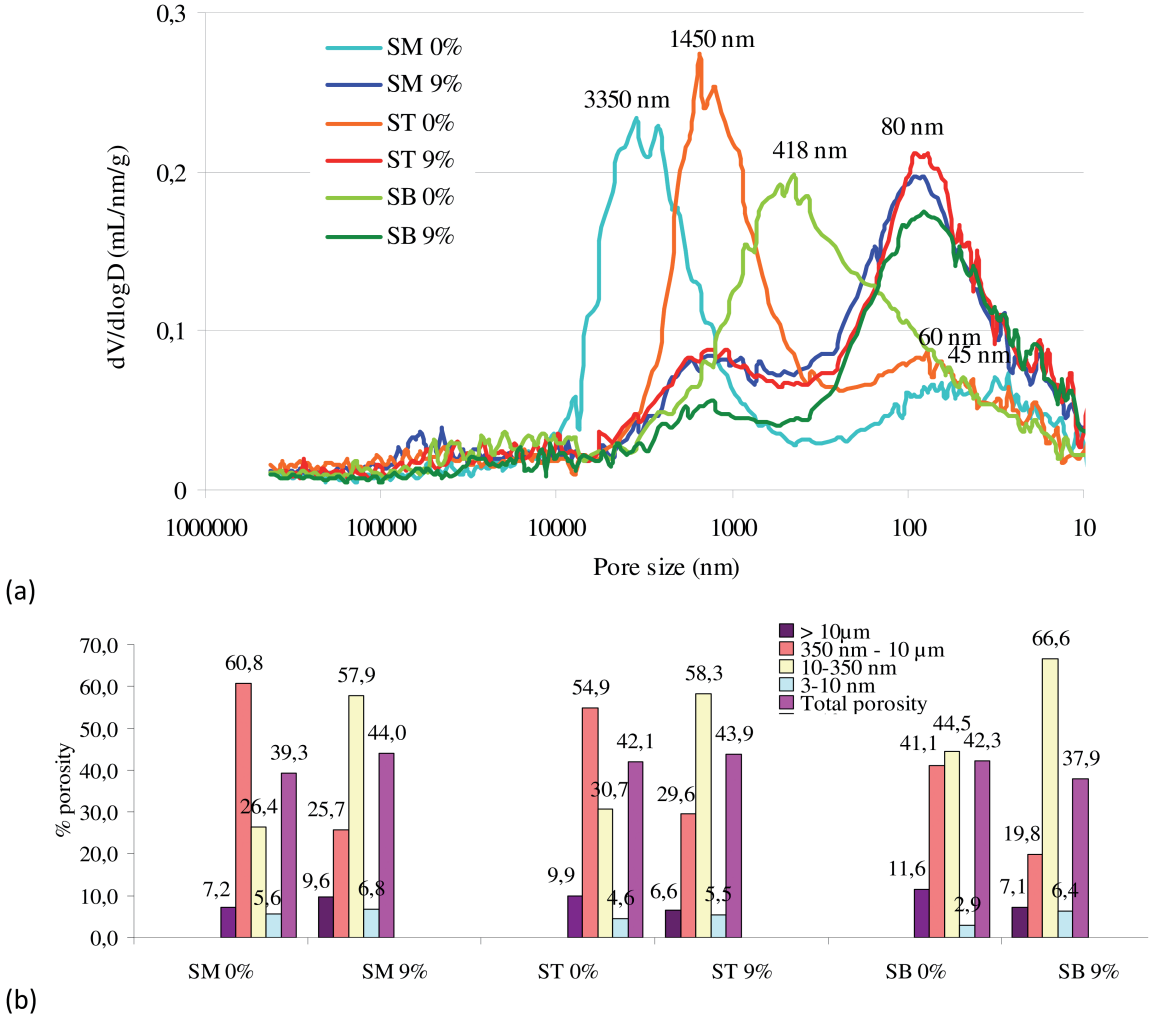

Fig. 3 - Measurements by mercury intrusion porosimetry (a) cumulative pore size distributions (PSD) curve and (b) Total porosity (%) and percentages of nanopores (3-10 nm), micropores (10-350 nm) and macropores (350 nm-10 µm) in the total pore volume

total porosity (Fig. 3b) close to 37-44%. The cement treatment of soils SM and ST resulted in an increase of several percents of the total porosity, whereas, in soil SB, it seemed to collapse the microstructure by decreasing the total porosity from 42.3% to 37.9%.

The effect of cement treatment on methylene blue value and Atterberg limits

The aim of the methylene blue test is to identify the reactivity of the clay fraction contained in soil, by measuring its ability to absorb methylene blue (MB) molecules. Considering its positive charge, the methylene blue molecule is attracted by the permanent negatively charged clay surfaces. The change of clay surface charge or surface accessibility to MB molecule impacts the methylene blue value (Vbs).

Even if the tested soil is not previously cement treated and compacted (that prevent soil from curing effect), the methylene blue test applied on a diluted suspension of cement and soil help to understand what happens in the cement-treated soils.

The results of Vbs measured on untreated soil and the soil-cement mixtures with different cement contents are shown in Fig. 4. The Vbs values vary inversely to the percentage of cement in the mixture. The Vbs value decreases by 85% for soil SB (between the untreated soil and the soil-cement mixture with 9%, of cement) while this rate was around 70% for ST and SM soils. As for Vbs, the change of Atterberg limits after cement addition only evidenced a short-term effect, with no effect of either curing (appearance of hydrated products) or microstructure (compaction). Atterberg limits on untreated soils and on soil-cement mixtures demonstrated regular decrease or increase in Fig. 4. The plastic limits of the 9% cement treated soils were increased by around 33% compared to the untreated soil. In accordance with literature results (Al-Rawas *et alii*, 2005; Horpibulsuk *et alii*, 2010; Nelson & Miller, 1992), the liquid limits as well as the plastic index strongly decreased by around 26% and 61% for soil ST, by 33% and 75% for soil SM and by 37 and 80% for soil SB. The effect of the stabilizer is stronger in soil SB that contains the lowest clay fraction compared to soils SM and ST.

These features helps to explain how the cement addition contributes to stabilize the expansive soils. The decrease of the surface along which the methylene blue molecules can adsorb (responsible of the decrease of Vbs) should induce a decrease of the swelling potential. However, the methylene blue test is applied on diluted suspension of soil and cement, while the cement treatment

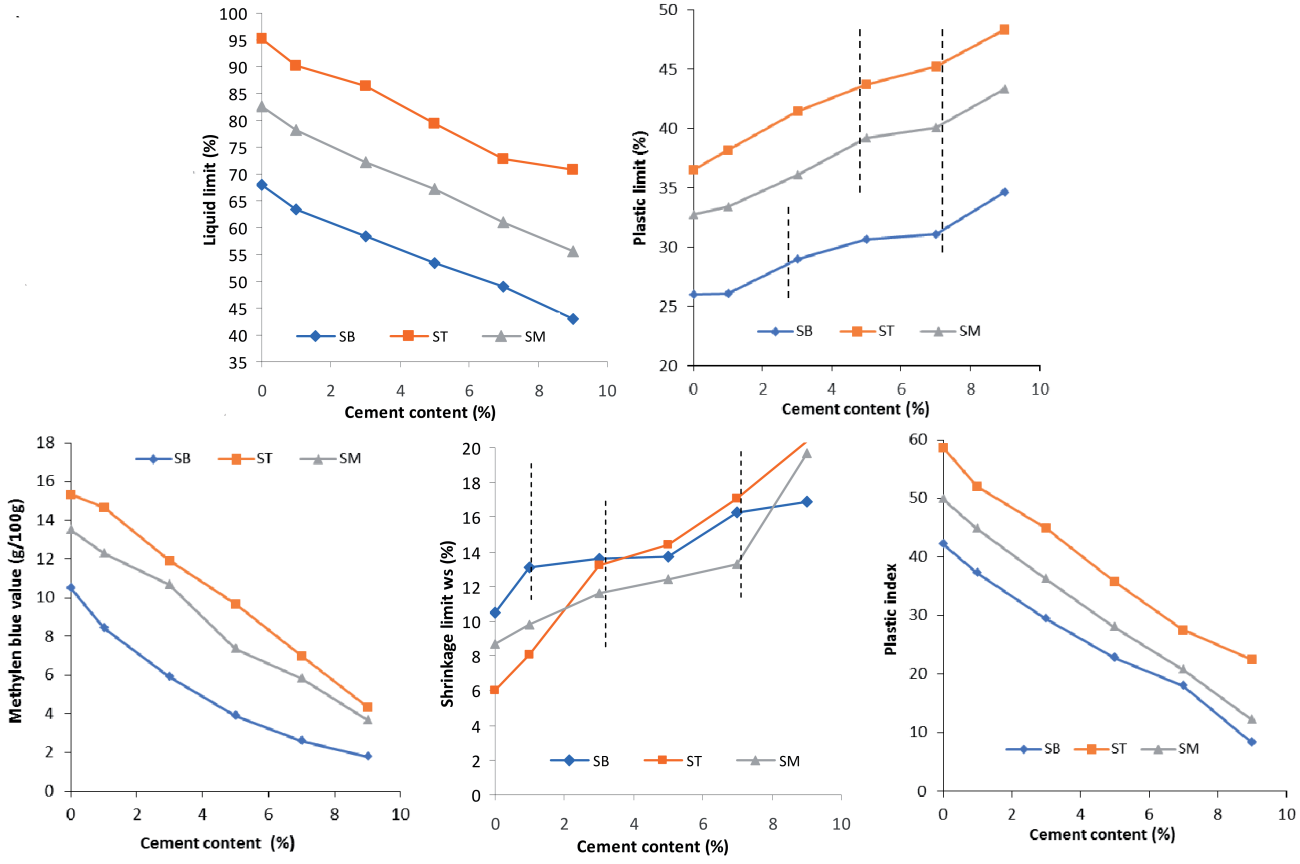

Fig. 4 - Atterberg limits, shrinkage limits and methylene blue values measured on untreated and cement treated soils SB, SM, and ST

concerns a compacted specimen with a lower water content, with a specific microstructure and a curing phase that results in the development of new mineral phases. The methylene blue test as well as Atterberg limits illustrates the short-term effect of the cement on the soil minerals. First, the cement addition makes the soil pH increase until alkaline pH range. This increase is compensated by the consumption of OH^-, useful to dissolve the soil particles and to trigger the pozzolanic reactions occurring at long term in compacted soils or in cement that contain blast furnace slags. The soil particles (especially clays) in alkaline medium acquire a more negatively charged surface, especially on their edges, which results in a higher adsorption of MB molecules and an increase of Vbs. This effect is neglected considering the low quantity of edge surfaces compared to permanent negatively charged basal surface. The effect of alkaline pH on MB molecule aggregation is also neglected. Indeed, a higher amount of adsorbed aggregates (named H-type) may be observed on some MB-clays (Chen, 2016).

On the other hand, the cement CEM II, with more than 65% of clinker, released Ca^{2+} cations during hydration, as observed with a lime addition. However, the cement effect is considered weaker than the lime effect (Okyay & Dias, 2010). The adsorption of Ca^{2+} by swelling clays occurred through cations exchange in the clay interlayer space, which results in the collapse of the clay structure and the decrease of the clay swelling potential (Konan, 2006). So, a decrease of the MB adsorption as well as the Vbs is expected.

In a compacted cement-treated soil, the lower water content (compared to the condition imposed in methylene blue test) slows down the Ca^{2+} mobility and its exchange on clay surface. This reduces the Ca^{2+} effect on soil, reinforced by the local competition between Ca^{2+} adsorption by clays and the portlandite $Ca(OH)_2$ or calcium silicate hydrate (or C-S-H) precipitation. Furthermore, after treatment and curing, the decrease in Vbs should be reinforced by the soil microstructure changes due to the C-S-H formation. Indeed, the pore accessibility becomes more difficult, so the accessible surface of minerals by water decreases. This change should also contribute to the decrease in Vbs observed in the treated soil after curing.

Now, the rate of the Vbs decrease observed on Fig. 4 slowed down from 7% of added cement especially for soil SB. It indicated a optimum cement content that corresponds probably to the saturation of the clay surface by calcium ions brought by cement. This quantity varies from a soil to another in accordance to its cation exchange capacity or CEC, linked to the soil mineralogy. Supplementary cement addition could no longer modify the charge of the particle or the water accessible surface of clay. This saturation was visible on Vbs curves of soil SB that reached earlier the saturation compared to soil SM and ST, because of its lower montmorillonite content (almost half that of soils ST and SM).

On the hand, PI, LL and PL curves didn't demonstrate stable values at high cement content even for soil SB. Such difference may come from the fact that Vbs is applied on suspension and Atterberg limits on paste or compacted soil for shrinkage limit. Atterberg limit (especially PL) demonstrated a slight intermediate stabilization before an new increase from the 7% identified as optimum cement content. This behavior is particular clear on shrinkage limit w_S (measured on specimen submitted to shrinkage test after a free swelling test). Three zones of differentiated behavior are proposed from PL or w_S curves and will be discussed later to explain swelling behavior.

The effect of cement treatment on cohesion and friction angle from shear test

The results of the direct shear tests in Fig. 5 shows that both the consolidated drained cohesion *c'* and the friction angle ϕ'

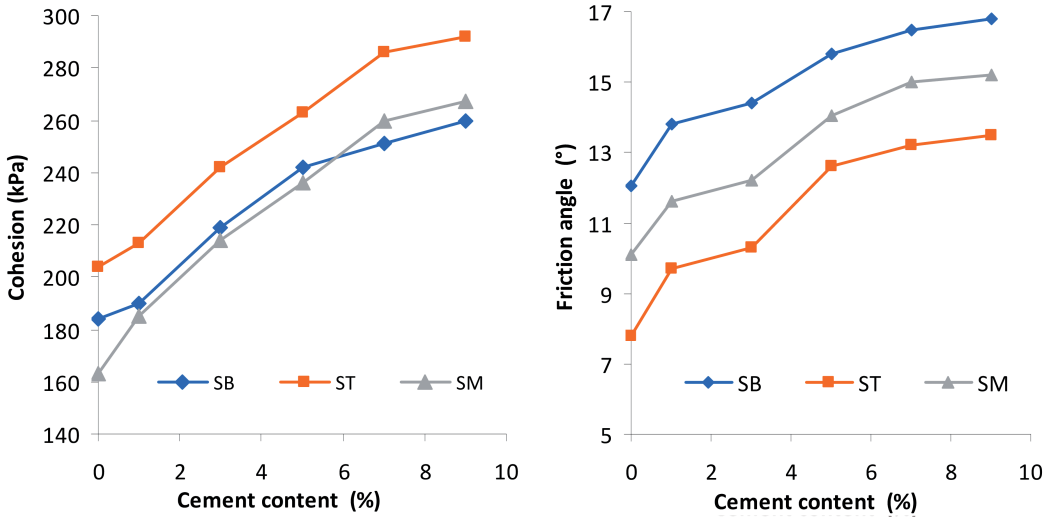

Fig. 5 - Effect of the addition of cement on the shear parameters c' (cohesion) and ϕ' (angle of friction) of soils SM, ST and SB

of the compacted soil specimens under unsaturated state were modified by the addition of cement. The cohesion *c'* and the angle of friction ϕ' increased first slowly and then proportionally to the added cement content (*Ac*) according to Eq. [1] and Eq. [2], respectively.

$$c' = 10\,Ac + 190 \quad (1)$$

$$\phi' = 0.5\,Ac + 10 \quad (2)$$

The cement treatment led to an increase in shear strength of all soils, resulting in an improvement of the bearing capacity of the soils. After a gradual increase, the cohesion c' and the angle of friction ϕ' obtained for 7% and 9% of added cement converged in a significant way. This behaviour agreed with the Vbs behaviour and it suggests a technical and economical optimum reinforcement for 7% of added cement. Khemissa *et alii* (2017) obtained quite similar results on drained shear test. Their data showed a higher dispersion which avoid to clearly observe a rigorous continuous increase of c' and ø' but an optimum cement content around 8% was determined. They observed also a decrease of *c'* and ϕ' after optimum when they tested cement content until 12% (the present study is limited to 9%).

If Khemissa *et alii* (2017) didn't propose any explanation for an optimum cement content, the tendency of *c'* and ϕ' as well as Vbs to reach a plateau for similar cement addition suggests that the saturation of clay by adsorbed Ca^{2+} brought by cement (as observed on Vbs at short term) governs the shear test results used to characterize the soil strengthening after treatment and curing.

The effect of cement treatment on the proctor optimum characteristics

The standard Proctor test was performed according to the standardized procedure on intact soils (sieved at 20 mm and dried at maximum 40°C) and on all soil-cement mixtures (with 1%, 3%, 5%, 7% and 9% cement content). The dry unit weights were determined immediately after compaction at each water content (without curing period), so as to draw the Proctor curves presented in Fig. 6.

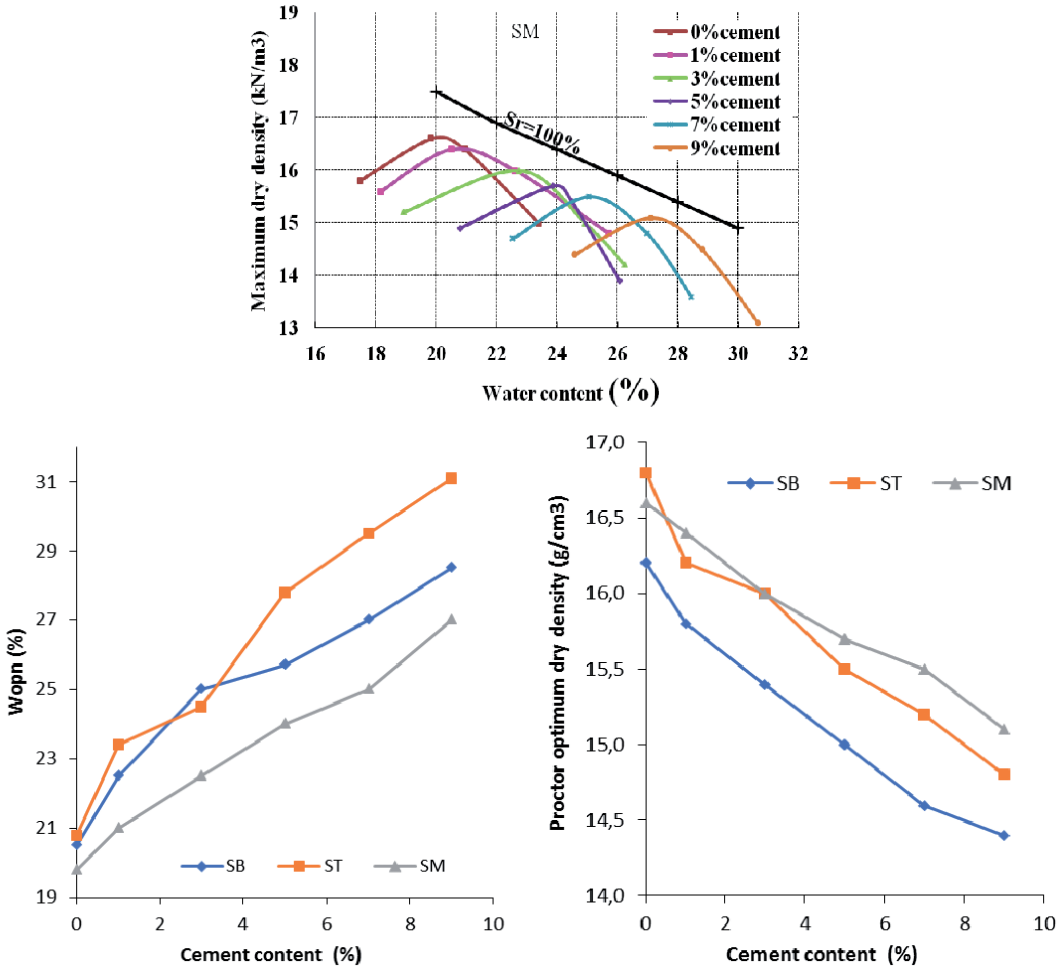

Fig. 6 - Effect of cement content on normal Proctor curves on SM (similar results obtained on soil SB and ST) and proctor water content and dry density versus the percentage of added cement

The untreated soils SB, SM and ST reached maximum dry densities of 16.2 kN/m^3, 16.6 kN/m^3 and 16.8 kN/m^3, respectively (see Tab. 3), with optimum water contents of 20.5%, 19.8% and 20.8%, respectively. After treatment, the soils SB, SM and ST showed similar change with a drop in their maximum dry densities down to 14,4 kN/m^3, 15.1 kN/m^3 and 14.8 kN/m^3, respectively, and an increase in their optimum water contents until 28.5%, 27% and 31.1%. The Proctor optimum of cement-treated specimens seems to keep the same saturation state, whatever the cement proportion. This feature is typical of soil-cement mixtures (Okyay *et alii*, 2010; Horpibulsuk *et alii*, 2010) or of soil-lime mixture (Di Sante *et alii*, 2014; Osinubi, 1998). Khemissa *et alii* (2017) demonstrated also that the maximum dry density as well as the optimum water content slightly decreased irregularly with cement addition (from 19.4 to 16.8% and from 16.2 to 15.1 kN/m^2 for 0% to 12% of added cement CEM II B respectively).

The incorporation of cement in soil leads first to a rapid aggregation of soil particles because of Ca^{2+} release. This aggregation also explains the decrease in Vbs previously observed. Nevertheless, the effect of cement addition remains lower than that of lime addition (Lemaire *et alii*, 2013). Macropores (> 10 μm) were probably formed after the dynamic compaction of aggregates of soil during the Proctor test, but could not be observed in statically compacted soils on Fig. 3a, because of the initial 80 μm grinding of the soil. The clay micropores collapsed locally in presence of Ca^{2+} ions, especially at the periphery of the blocks of soil. Calcium ions cannot easily migrate into the soil mass because of the low water content that reduces their diffusion rate. This situation should be more uniform in statically compacted soils, after initial grinding (as used for shear test or swelling-shrinkage test). Pores were filled by hydrated products from cement hydration coupled to the development of the internal nanoporosity of the new precipitated phases. Both phenomena resulted in soil strengthening at short and long term. Consequently, the cement treatment resulted in lower dry density of the specimen, whatever the soil preparation. This conclusion is confirmed by the decrease in macroporosity measured by MIP on statically compacted soils in Fig 3b. Finally, the dry density versus the cement for soil SB showed in Fig. 6 a plateau from 7% of added cement. This result is in agreement with the behaviour of Vbs, c' and ϕ' curves, while the Proctor optimum water content followed slightly a *S*-curve without stabilization at high cement content.

The effect of cement treatment on shrinkage curves

To investigate the decrease of the soil deformation and its strengthening after cement treatment, the specimens were submitted to a free swelling test until reaching the maximum moisture content w_{max}, followed by a shrinkage test whose results are drawn in w-e plan on Fig. 7.

The maximum water content at the end of the free swelling (Fig. 7d) (corresponding to the beginning of the shrinkage test) appeared significantly impacted by the quantity of added cement. The adsorbable water by soil decreased with the collapse of the pores under the calcium effect and the precipitation of hydrated products. But, the maximum water content may also increase after wetting-drying cycles applied on specimen because of the change in microstructure, notably the gradual breaking of the cemented or carbonated structure.

The shrinkage curves starting at e_{max} (for w_{max}) in Fig. 7, appeared to be shifted far from the saturation line (the shift corresponds to 'de'). The soil microstructure resulting from remolding with or without cement addition followed by compaction, is at the origin of the shift that decreased with the increasing cement addition in mixture. It is in relation with the decrease of the micropores after treatment.

Both the air entry point wa (defined as the water content from which the shrinkage curve no longer follows the slope of the saturation line) and the shrinkage limit w_S (corresponding to the moisture content under which the soil deformation does no longer change) increased with increasing cement addition. The shrinkage limit of soils SB, SM and ST varied from 10.5%. 8.7% and 6 % with no treatment to 16.3%. 19.7% and 20.4% with 9% cement treatment. Such behavior demonstrated the stiffening of the soil microstructure that could no longer deform even if the water content diminished.

The effect of cement treatment on the soil swelling and total soil deformation

The Figure 8 shows the evolution of the free swelling strain $S = \Delta H/H_o$ as a function of time for the three cement treated soils. The swelling potential $S = \Delta H_{max}/H_0$ was measured at the end of the free swelling test, after an equilibration of 15 to 21 days.

The longer time was required for untreated soils while treated soils reached the maximum swelling amplitude after only 2 weeks. The slope of the swelling curve of untreated soils changed gradually with variable slope. The first slope (low rate of swelling) corresponded to a rapid hydration of the soil particles by intrusion of hydrated cations. It was followed by a intense swelling of clay sheet reinforced by osmosis phenomenon. This second slope corresponded to the saturation of micropores and interlayer spaces. Then, the swelling rate decreased during a few days until it reached a slow rate at longer time (third slope). Water keeps on its intrusion into pores and in interlayer spaces in order to form several water layers until the beginning of the clay dispersion after the weakening of bounds between particles.

Cement treated soils behaved slightly differently with the extension of the hydration phase (without intense swelling), followed by the shortening of the second swelling phase that stopped abruptly when the third slope (almost zero) starts. The soil strengthening (cementation) that prevents the pores and

aggregates deformation (or reorganization) is at the origin of the change of behavior.

After the monitoring of the swelling slopes, the swelling pressures σ_s (kPa) of the treated and untreated soils were measured by loading swelled specimens, to bring them back at their initial void ratio. The values of S (%) and σ_s (kPa) are drawn in Fig. 9.

The increase in cement content in soil-cement mixtures with all soils (SM, ST or SB) reduced the swelling potential S (%) up to 79% for soils with 9% of added cement. The same results were obtained for the swelling pressure σ_s (kPa), with a reduction greater than 70% which confirms previous results of Nalbantoglu & Gucbilmez (2001) and Al-Rawas *et alii* (2005). The swelling potentials were in accordance with the montmorillonite content and the total clay content, and with the classifications of expansive soils in which the three soils are characterised by high to very high swelling level.

The swelling pressures or potentials versus the cement content on Fig. 9 were fitted by S-curves with various curvatures (third degree polynomial fitting), contrary to the exponential fitting proposed by Mahamedi & Khemissa (2013). The swelling potential curves demonstrated a final decrease for higher cement content than 7% after an intermediate stabilization as observed on PL ou ws curve in Fig. 4. A the opposite, the curves of swelling pressures followed the same trend as observed previously for Vbs, c' or , ø' i.e. a stabilization from the optimum cement content around 7%.

To discriminate the effect of cement addition on swelling potential from the effect of the initial water content and the density of the specimen, the total soil deformation $S_{tot}(\%)=\Delta V_{tot}/V_0$ was also measured. Indeed, lower swelling is observed in soil with looser and/or wetter initial state. The decrease in initial densities and the increase in initial water content of statically compacted treated specimens with increasing cement contents (as showed for example on SM soil in Tab. 6), contribute to the decrease of the swelling potential. The measurement of the total soil deformation

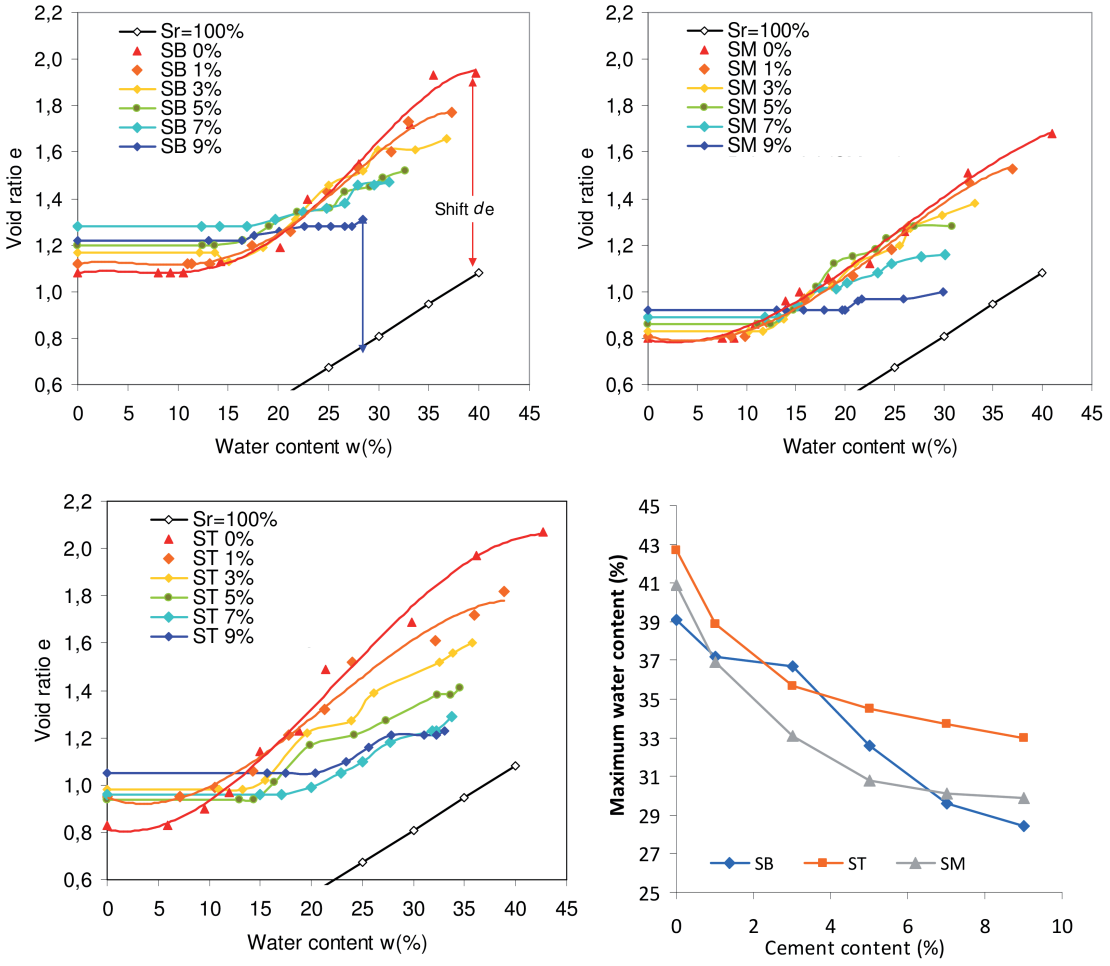

Fig. 7 - Effect of cement addition on the shrinkage curve after free swelling of soils (a) SB, (b) SM, (c) ST and maximum water content versus the cement content (d)

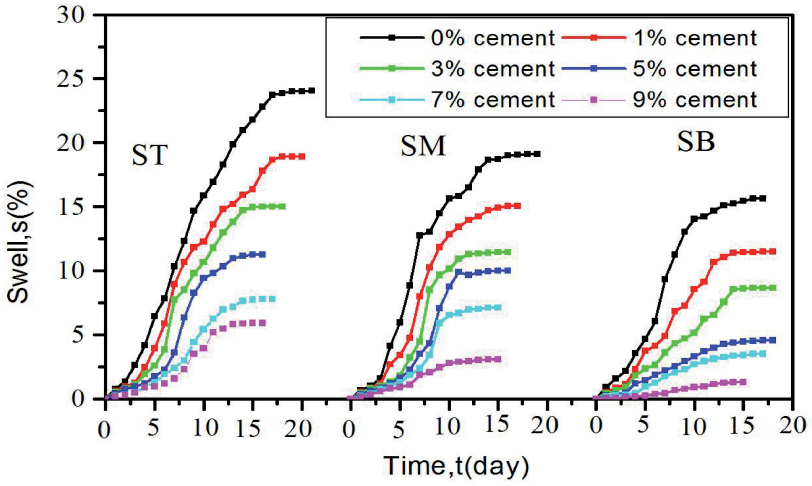

Fig. 8 - Effect of cement addition on the swelling potential versus time for soils SB, SM and ST

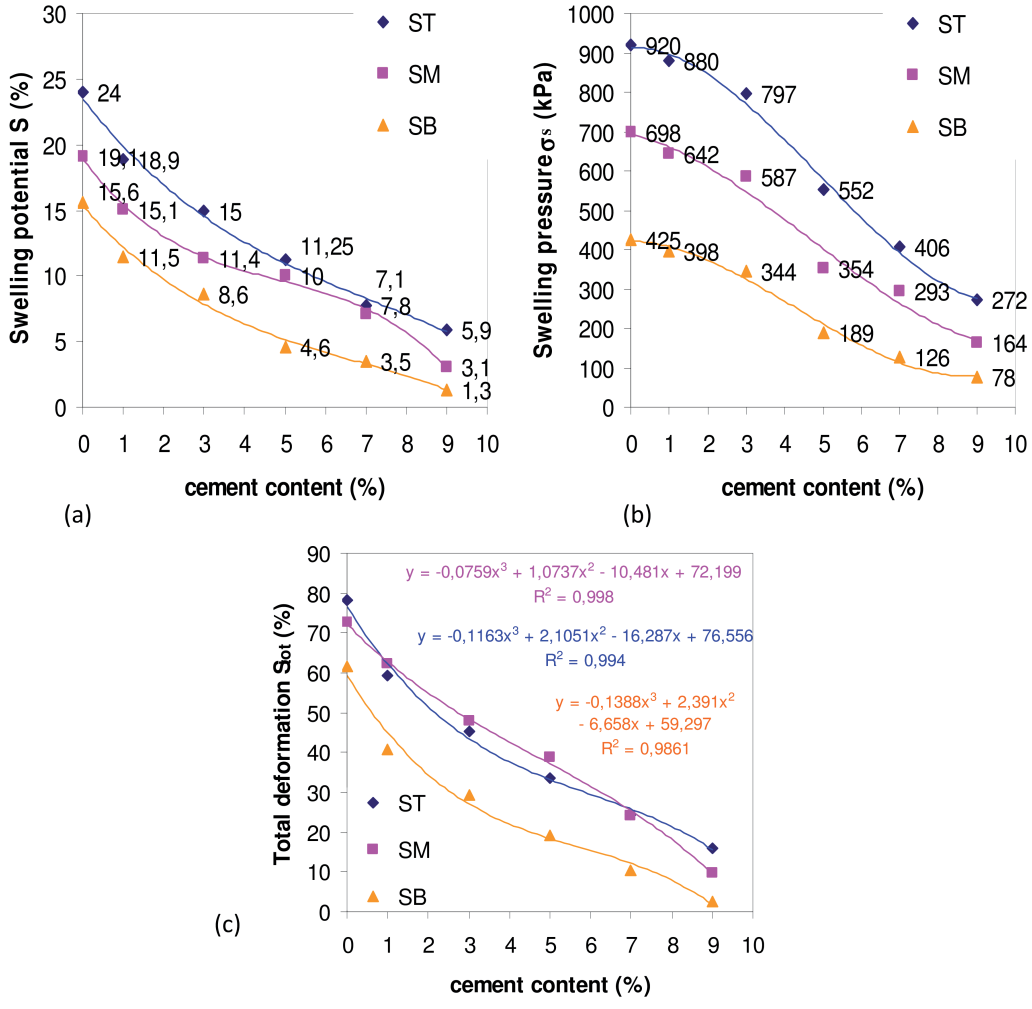

Fig. 9 - (a) Swelling potential, (b) swelling pressure and (c) total deformation of soil during shrinkage test after free swelling test, versus cement addition for soils SB, SM, and ST

S_{tot} (%) from shrinkage test after free swelling test will be used to avoid this disturbing effect.

S_{tot} (%) corresponds to the volumetric shrinkage deformation between w_{max} (after swelling) and the dry state. Such characteristic can be considered as an intrinsic soil parameter, contrary to the swelling or shrinkage potentials that vary with the initial water content of tested specimen. On Fig. 9c, S_{tot} (%) dropped with higher cement content (only small cracks were detected on untreated or treated specimen after shrinkage which validated the measurement of volumes).

The total soil deformation followed a *S*-curve, such as the swelling potential. A third degree polynomial function fitted well the curves for the three soils with quite close parameters. The last parameter of the function controls the vertical shift of the curve. The shift is particularly clear for the most carbonated soil SB, while the soils ST and SM (the richest in clay) had quite similar total shrinkage deformation versus the added cement. Results suggest that total soil deformation after cement treatment could be approximated by a common equation correlated to the position of the limits of three swelling zones that correspond to the zones observed on PL or w_S curves. Zone I corresponds to a significant increase in w_S in Fig. 4 (the swelling potential remains important but the cement has not yet played its stabilizing role). Zone II corresponds to a plateau where ws slightly increases, with a low swelling reduction (it's the beginning of the stabilizing effect until the soil saturation) and zone III shows a new significant increase in shrinkage limits. Then, the swelling is decreased until zero with the strengthening of the structure, which results in the increase of its mechanical characteristics (a continuous cemented matrix can be formed once a certain quantity of added cement).

The equation and the limits of each zone depend especially on mineralogy (clay content, swelling clay content, non-clay content especially carbonate content…) or physical soil parameters. The testing on a larger set of soils should help to discriminate with accuracy the most adequate parameters to describe the total soil deformation and the position of the three swelling zones.

CONCLUSIONS

The effects of cement treatment at various proportions (1%, 3%, 5%, 7% and 9%) on the properties of three soils were investigated by using physico-chemical and mechanical tests. Results confirmed that cement treatment improves the geotechnical and mechanical characteristics of the soils, notably by increasing the cohesion and friction angle, hence increasing the shear strength and the bearing capacity of the cement treated soils.

The plastic limit PL and the shrinkage limit w_S, increased with the cement content, while the liquid limit LL, the plasticity index PI, the swelling potential *S* (that depends on the initial water content and densities of compacted specimen), the total shrinkage deformation after free swelling S_{tot} (a more intrinsic characteristic of soils independent to the initial soil moisture), as well as the swelling pressure σ_s decreased. A cement treatment at 9% reduced the swelling potential by 75 to 91% for tested soils, corresponding to a decrease in swelling pressure by 70 to 81%. Furthermore, the Proctor optimum water content increased while the optimum densities decreased with the cement content in treated soils. Moreover, the total soil deformation after cement treatment can be approximated by an equation correlated with the position of two limits observed on the curves w_s (or PL) versus the percentage of added cement. These two limits reveal the existence of three swelling zones. Zone I corresponds to a significant increase of the shrinkage limit with a high swelling potential, but the cement addition has not yet played its role of stabilizer. Zone II corresponds to a plateau where the shrinkage limit slightly increases, accompanied by a slight reduction in swelling. This is the beginning of the effect of the stabilizer. Zone III shows a new significant increase in shrinkage limits. The swelling is reduced to zero with the strengthening of the structure.

In order to interpret the data, the specimen preparation impacting the soil microstructure and the C-S-H development, the specimen mineralogy (the clay fraction interfered with cement hydration but favoured the long term pozzolanic reaction), as well as the effect of cement hydration (that introduced calcium ions in soil) are important parameters to consider. The microstructural approach of soil cement treatment agreed with the idea that cement acted as a flocculating agent on the short term, but with a poor efficiency compared with lime. Indeed, cement treatment reduced the water sensitivity of clay particles due to the effect of calcium ions. This flocculating effect explained the decrease of swelling amplitude, methylene blue value (Vbs) or plasticity index. The Vbs determined on the soil particles without curing period is sensitive to the flocculating effect of cement addition, that reached a maximum depending on the clay content, and corresponding to the Ca^{2+} saturation of clays. The Ca^{2+}-saturation of soil particles explains partially why the Vbs reached a minimum for a cement addition of 7-8% in tested soils. This maximum coincided also with the cement content required to reach the maximum value of c' and ϕ'.

Conversely, the shrinkage limits w_S, swelling pressures σ_s, total shrinkage deformations after swelling S_{tot}, swelling potentials *S*, cohesions c' and friction angles ϕ' were measured after a 28 days curing period on statically compacted specimens of soils previously ground at 80 µm and intimately mixed with cement. In this case, the soil microstructure played a determining role. The cement distribution in statically compacted specimens (different from that in dynamically compacted specimen for proctor test) impacted the C-S-H development and the efficiency of the strengthening. On the long term, cement bound the clay aggregates together thanks to precipitated hydrated products such as calcium silicate hydrate that modified the pore repartition, and was at the origin of the soil stiffening accompanied by a decrease in density.

REFERENCES

ASTM D4546-96 (1996) - *Standard test methods for one-dimensional swell or settlement potential of cohesive soils.*

AFNOR NF P11-300 (1992) - *Earthworks. Classification of materials for use in the construction of embankments and capping layers of road infrastructures.*

AFNOR NF P94-051 (1993) - *Determination of Atterberg's limits. Liquid limit test using Casagrande apparatus. Plastic limit test on rolled thread.*

AFNOR NF P94-050 (1995) - *Determination of moisture content. Oven drying method.*

AFNOR NF P94-093 (2014) - *Determination of the compaction reference values of a soil type - Standard proctor test - Modified proctor test.*

AFNOR NF P94-056 (1996) - *Granulometric analysis. Dry sieving method after washing*.

AFNOR NF P94-057 (1992) - *Granulometric analysis. Hydrometer method.*

AFNOR NF P94-048 (1996) - *Determination of the carbonate content - Calcimeter method.*

AFNOR NF P94-071 (1994) - *Direct shear test with shearbox apparatus. Part 1 : direct shear.*

Al-Mhaidib A.I. (2006) - *Swelling behavior of expansive shale: a case study from Saudi Arabia.* In: Al-Rawas A.A. & Goosen M.F.A. (Eds.). *Expansive soils: recent advances in characterization and treatment.* Taylor & Francis Group, 273-287.

Al-Rawas A.A., Hugo A.W. & Al-Sarmi H. (2005) - *Effect of lime, cement and Sarooj (artificial pozzolan) on the swelling potential of an expansive soil from Oman*. Build. Environ., **40**: 267-281.

Petry T.M. & Little D.N. (2002) - Review of Stabilization of Clays and Expansive Soils in Pavements and Lightly Loaded Structures - History, practice and future. Journal of Materials in Civil Engineering, **14** (6): 447.

Bekkouche A., Djedid A., Mamoune S.M. & Zoubir A. (2003) - *Esquisse de la carte géotechnique du groupement Tlemcen-Mansourah-Chetouane.* Implication de la géotechnique dans le développement Marrakech, Maroc.

Belabbaci Z., Mamoune S. & Bekkouche A. (2012) - *Laboratory study of the influence of mineral salts on swelling*. Earth Science Research Journal, **2** (2): 135-142.

BRE-UK (1980) - *Classification of swelling soil.* Building Research Establishment United Kingdom.

Chen F.H. (1988) - *Foundations on expansive soils.* Developments in Geotechnical Engineering, Elsevier, 463 pp.

Chen C.W. (2016) - *Mineralogical approach to use the non-qualified fine aggregates in asphalt concrete pavement*. Ph.D thesis University Paris Est, France.

Chew S.H., Kamruzzaman A.H.M. & Lee F.H. (2004) - *Physico-chemical and engineering behavior of cement treated clays.* Journal of Geotechnical and Geoenvironmental Engineering, **130** (7): 696-706.

Choquette M., Marc A-B. & Locat J. (1987) - *Mineralogical and microtextural changes associated with lime stabilization of marine clays from eastern Canada*. Applied Clay Science, **2** (3): 215-232.

Dakshanamurthy V. & Raman V. (1973) - *A simple method of identifying an expansive soil*. Soils and Foundations, **13** (1): 97-104.

Derriche Z. & Lazzali F. (1997) - *Analyse des mécanismes de stabilisation d'un sol gonflant par apport de chaux sous différentes formes.* In: Marinos P.G, Koukis G.C., Tsiambaos G.C. & Stournaras G.C. Engineering Geology and the Environment, Vol. 1: 79-84.

Di Sante M., Fratalocchi E., Mazzieri F. & Pasqualini E. (2014) - *Time of reaction in lime treated clayey soil and influence of curing conditions on its microstructure and behaviour*. Applied Clay Science, **99**: 100-109.

Gueddouda M.K., Goual I. & Benabed B. (2013) - *Effet de chaux, ciment et sel sur le potentiel de gonflement des argiles gonflantes des régions arides en Algérie.* European Journal of Environnemental and Civil Engineering, **17** (5): 315-328.

Hachichi A., Bourokba S.A. & Fleureau J.M. (2007) - *Stabilisation chimique de deux sols gonflants de la région d'Oran*. Revue Française de Géotechnique, **118**: 3-11.

Horpibulsuk S., Rachan R., Chinkulkijniwat A., Raksachon Y. & Suddeepong A. (2010) - *Analysis of strength development in cement-stabilized silty clay from microstructural considerations.* Construction and Building Material, **24**: 2011-2021.

Chew S.H. & Lee F.H. (2006) - *Microstructure of cement-treated Singapore marine clay.* Ground Improvement, **10** (3): 113-123.

Khattab S.A., Al-Mukhtar M. & Fleureau J.-M. (2007) - *Long-term stability characteristics of a lime-treated plastic soil.* Journal of Materials in Civil Engineering, **19** (4): 358-366.

Konan K.L. (2006) - *Interaction entre des matériaux argileux et un milieu basique riche en calcium.* Ph.D thesis University Limoges, France.

Khemissa M. & Mahamedi A. (2014) - *Cement and lime mixture stabilization of an expansive overconsolidated clay,* Applied Clay Science, **95**: 104-110.

Khemissa M., Mahamedi A. & Mekki L. (2017) - *Laboratory investigation of the treatment effects by hydraulic binders on the physical and mechanical properties of an overconsolidated expansive clay.* International Journal of Geotechnical Engineering, 1-14.

Khemissa M., Mekki L. & Mahamedi A. (2018) - *Laboratory investigation on the behaviour of an overconsolidated expansive clay in intact and compacted states.* Transportation Geotechnics, **14**: 157-168

Lamara M., Gueddouda M.K. & Benabed B. (2006) - *Stabilisation physico-chimique des sols expansifs, sable de dune avec du sel.* Revue française de Géotechnique, **115**: 25- 35.

Lamara M. & Gueddouda M.K. (2008) - *Comportement et remèdes des sols expansifs dans les régions arides.* Proceeding of symposium SEC2008 « Sécheresse et Construction », Paris, 329-335.

Lemaire K., Dennele D., Bonnet S. & Legret M. (2013) - *Effects of lime and cement treatment on the physico-chemical, microstructural and mechanical characteristics of a plastic silt.* Engineering Geology, **166**: 245-261.

Louafi B. & Bahar R. (2012) - *Sand: an additive for stabilization of swelling clay soils*. International Journal of Geoscience, **3**: 719-725.

Mahamedi A. & Khemissa M. (2013) - *Cement stabilization of compacted expansive clay.* Journal of Science and Technology, **3** (1): 33-38.

Mellas M., Hamdane A., Benmeddour D. & Mabrouki A. (2012) - *Improvement of the expansive soils by the lime for their use in road works.* Proc. 10th Int. Cong. Adv. Civ. Eng. Middle East Technical University, Ankara, Turkey, 1-8.

Miller G.A. & Azad S. (2000) - *Influence of soil type on stabilization with cement kiln dust.* Construction and Building Material, **14**: 89-97.

Nalbantoglu Z. & Gucbilmez E. (2001) - *Improvement of calcareous expansive soils in semi-arid environments.* Journal of Arid Environments, **47** (4): 453-463.

Nelson J.D. & Miller D.J. (1992) - *Expansive soils. Problems and practice in foundation and pavement engineering.* Department of Civil Engineering, Colorado State University, Wiley, New York, 259 pp.

Okyay U.S. & Dias D. (2010) - *Use of lime and cement treated soils as pile supported load transfer platform*. Engineering Geology, **114** (1): 34-44

Osinubi K.J. (1998) - *Influence of comparative efforts and compaction delays on lime-treated soil.* Journal of Transportation Engineering, **124** (2): 149-155.

Osula D.O.A. (1996) - *A comparative evaluation of cement and lime modification of laterite*. Engineering Geology, **42** (1): 71-81.

Seed H.B., Woodward R.J. & Lundgren R. (1962) - *Prediction of swelling potential for compacted clays*. Journal of Soil Mechanics and Foundation Division, **88**: 53-87.

Snethen D.R., Johnson L.D. & Patrick D.M. (1980) - A model for predicting expansive soil behavior. Proceedings, of the Fifth International Conference on Expansive Soils, Adelaide, 22–26.

Wang Y., Duc M., Cui Y.-J., Tang A.M., Benhamed N., Sun W.J. & Ye W.M. (2017) - *Aggregate size effect on the development of cementitious compounds in a lime-treated soil during curing*. Applied Clay Science, **136**: 58-66.

Williams A.B. & Donaldson G.W. (1980) - *Developments related to building on expansive soils in South Africa,* Proceeding of the 4th International Conference on Soil Mechanics and Foundation Engineering, Denver, 834-844.

Received May 2018 - Accepted November 2018